

Experimental Investigation of Creep Behavior of Reactor Vessel Lower Head

T.Y. Chu*, M. Pilch*, J.H. Bentz* and A. Behbahani**

*Sandia National Laboratories, **USNRC

CONF-980341--

1. INTRODUCTION AND BACKGROUND

The objective of the USNRC supported Lower Head Failure (LHF) Experiment Program at Sandia National Laboratories is to experimentally investigate and characterize the failure of the reactor pressure vessel (RPV) lower head due to the thermal and pressure loads of a severe accident. The experimental program is complemented by a modeling program focused on the development of a constitutive formulation for use in standard finite element structure mechanics codes. The problem is of importance because:

- lower head failure defines the initial conditions of all ex-vessel events;
- the inability of state-of-the-art models to simulate the result of the TMI-II accident (Stickler, et al. 1993); and
- TMI-II results suggest the possibility of in-vessel cooling, and creep deformation may be a precursor to water ingress leading to in-vessel cooling.

RECEIVED

MAR 12 1998

OSF

2. SCALING ANALYSIS AND EXPERIMENTAL DESIGN

A scaling analysis was performed (Chu et al., 1997) to ensure sub-scale experiments are properly designed. The key results are:

- the experimental apparatus should be geometrically scaled from a reactor pressure vessel to preserve the hoop stress;
- prototypical material should be used because with present knowledge, material creep behavior can not be scaled;
- the heat flux for the experiment should be scaled by the experiment scale to preserve the temperature history.

3. EXPERIMENTAL APPARATUS

The apparatus is basically a scaled version of the lower part of a TMI-like reactor pressure vessel (RPV) without the vessel skirt, consisting of a SA533B1 steel hemispherical head, and a 30-cm vertical section replicating the lower part of the RPV cylindrical wall, see Figures 1. The inner-diameter of the lower head is 0.91 m corresponding to a geometrical scale factor of 4.85. The wall thickness is typically 30 mm. Due to the hot-spinning forming operation, the wall is slightly thicker at the equator.

A hemispherical heater with nine independently controlled segments is used to simulate the energy transfer from the core debris to the reactor vessel, see Figures 1 and 2. The inner surface of the lower head is coated with Pyromark[®] black paint for efficient radiation absorption. The outer surface of the lower head and the inner surfaces of the cylindrical section and the top flange are insulated. A cooling band near the bottom of the cylindrical section provides the proper far field temperature condition (due to the presence of water in the RPV). The pressure load is provided by a manifold of bottled argon, and controlled by automatic fill and bleed valves.

DISTRIBUTION OF THIS DOCUMENT IS UNLIMITED

MASTER

19980420070

DISCLAIMER

This report was prepared as an account of work sponsored by an agency of the United States Government. Neither the United States Government nor any agency thereof, nor any of their employees, makes any warranty, express or implied, or assumes any legal liability or responsibility for the accuracy, completeness, or usefulness of any information, apparatus, product, or process disclosed, or represents that its use would not infringe privately owned rights. Reference herein to any specific commercial product, process, or service by trade name, trademark, manufacturer, or otherwise does not necessarily constitute or imply its endorsement, recommendation, or favoring by the United States Government or any agency thereof. The views and opinions of authors expressed herein do not necessarily state or reflect those of the United States Government or any agency thereof.

Initially, the vessel is filled to approximately half of the desired pressure, and the vessel pressure increases with heating. When the vessel reaches 800 K, the vessel pressure is set at the desired testing pressure and is maintained at that pressure while the vessel is heated to failure.

The shape and the local wall thickness of the vessel are measured before and after the experiment using a grid system defined by punch marks on the vessel surface. A computerized mapping device, based on the tracking of a manually positioned pointer, was used in mapping the vessel shape. An ultrasonic thickness gage was used for vessel wall thickness measurements. Locations on the hemisphere are described in terms of "longitude" and "latitude." The equator of the bottom head is 0° latitude and the bottom center of the lower head is 90° latitude.

Arrays of thermocouples are used to measure inner and outer wall temperatures. Linear displacement transducers deployed along a chosen longitude, at typically 3-5 latitude locations, are used to monitor the deformation of the test vessel. Except for the bottom center of the lower head (90°), there are two transducers at each location, one for vertical displacement, and one for horizontal displacement. X-ray is also used to monitor real-time profile of the test vessel.

4. EXPERIMENTAL RESULTS

The results of the first five experiments out of the planned eight-experiment series are reported here. The main variables are heat flux distribution, vessel pressure, and the absence or presence of penetrations on the vessel bottom. All five experiments were performed with an internal pressure of 10 MPa corresponding to a hoop stress of 75 MPa in the vessel wall.

4.1 LHF-1 Experiment - Uniform Heating and No Penetrations

The lower 60° (latitude 30° to 90°) of the vessel wall was heated uniformly in LHF-1. Representative temperature and displacement histories of the vessel wall are shown in Figure 3. Significant increase of the creep rate was observed at about 120 minutes into the test at a vessel temperature of approximately 930 K. As the wall temperature increased, the creep rate continued to accelerate. The vessel failed catastrophically at 145 minutes into the test; at a vessel temperature of 1011 K. The recorded displacement at vessel bottom center at the time of failure was 0.12 m.

As shown in Figure 4, the vessel failed non-symmetrically with respect to the 90°/270° plane. The 180° longitude (left side) profile shows more deformation than the 0° profile. The deformation is relatively symmetrical with respect to the 0°/180° plane. The shape of the failure is approximately oval, measuring 0.49 m by 0.25 m. The hole opening corresponds to the material bounded approximately by latitude 66° and 80°, and longitude 110° and 240°. Post-test inspection indicates that the initial failure occurs at approximately 150° longitude/66° latitude. Examination of the pre-test and post test thickness maps of the vessel, Figures 5 and 6, suggests that the failure region corresponds to a region of slightly reduced wall thickness in the pre-test vessel, and the thin section "attracts" deformation during vessel creep.

The overall extension of the vessel was approximately 16-cm, corresponding to an overall strain (based on the vessel outer radius) of 33%. The linear strain near the failure location was found to be about 200% (distance between punch grid marks increased by a factor of 3), corresponding nicely with the 9(3²)fold wall thickness reduction, from 29 mm to 3 mm. The wall thickness along the edge of the failure varies from 3 mm to 16.5 mm. Based on these values, the linear strain at failure varies from approximately 34% to 200%.

4.2 LHF-2 Experiment - Center-Peaked Heat Flux and No Penetrations

LHF-2 has a center-peaked heat flux profile reminiscent of TMI-II. The initial LHF-2 heating schedule followed the same temperature history of LHF-1 up to 700K. Beyond 700K, the center region of the vessel (68°-90°) was controlled to follow LHF-1, and the surrounding region was maintained to be approximately 100K lower.

LHF-2 was completed in two runs due to heater failure. The experiment was interrupted approximately 180 minutes into the first run of the experiment with the bottom center section (68° to 90°) at approximately 1000K and experienced 7 cm of deformation.

Representative temperature and displacement histories of the vessel wall during the second run are shown in Figure 7; the displacements shown are values beyond that of the first run (7 cm at 90° and 5 cm at 70°). Figure 8 illustrates the center-peaked vessel temperature profile and the corresponding vessel yield strength distribution. The yield strength is based on a best fit of existing property values as a function of temperature (Pilch et al., 1998). Significant creep occurred at approximately 135 minutes and failure occurred at approximately 160 minutes into the second run. The corresponding wall temperature at creep initiation was in the range of 930-950 K. The vessel temperature at failure was in the range of 1000-1025 K.

The overall profile of the posttest vessel, as shown in Figures 9 and 10, was shaped like an inverted top half of a pear. The total vessel deformation was 16.7 cm. There is an inflection point in the 60°-70° region corresponding to the knee in the vessel yield strength profile, Figure 8. The failure is an oval approximately 4 cm by 7 cm, substantially smaller than the 25 cm by 49 cm of the LHF-1 failure. The minimum wall thickness at failure was approximately 3 mm, similar to LHF-1. The failure appeared to have initiated near 77° latitude and 205° longitude, and is bounded between 77° to 79° latitude and 200° to 210° longitude.

4.3 LHF-3 Experiment - Edge-Peaked Heat Flux and No Penetration

LHF-3 seeks to simulate the edge-peaked heat flux distribution due to coremelt convection. The initial heating schedule for LHF-3 was designed to follow essentially the same temperature history of LHF-1 up to approximately 800K; beyond this temperature, heater segments were adjusted to achieve an edged-peaked heat flux distribution centered around 34° latitude. The 34° location is the approximate coremelt level corresponding to 75% of the core of a typical PWR.

Representative temperature and displacement histories of the vessel wall

are shown in Figure 11. Figure 12 illustrates the edge-peaked vessel temperature profile and the corresponding vessel yield strength distribution. Significant creep occurred at approximately 140 minutes at a peak vessel temperature of 960K and failure occurred at approximately 160 minutes at a peak wall temperature of approximately 1000K. The measured deformation at failure, at the bottom center, was about 5 cm. The failure of LHF-3 is a nearly perfect latitudinal rip at 33.5°, coinciding with the location of the temperature peak, see Figure 13. The rip spans approximately 70° between 310° and 20° longitude. From the deformation of the grid pattern it is also quite obvious that the region of large strain is confined to materials surrounding the rip. An examination of the pre-test vessel thickness mapping indicated a region of reduced thickness between 250° and 360° longitude for the 30° to 40° latitude region of the vessel. There is a 50° overlap between the thin-wall region (250°-360°) and the failure region (310°-20°). It is interesting to note that the circumferential distribution of the peak temperature is uniform within 10K, but the low temperature/high strength region is near the 270° longitude. It is plausible that pre-test vessel wall thickness variation is still the precursor of vessel failure but the final failure configuration is modified by the 10K circumferential temperature variation.

4.4 LHF-4 Experiment - Uniform Heating with Penetrations

The purpose of the experiment was to examine the effect of penetrations on vessel failure. The vessel was uniformly heated. The penetration pattern was an exact scaled duplicate of the penetration pattern of a typical PWR in the region of 60° to 90° latitude of the lower head, see Figure 15. The range of angular location overlaps the expected region of vessel creep for a uniformly head lower head, based on the observations of LHF-1. The scaled Inconel penetration tube has a diameter of 8.2 mm. The largest diametrical clearance between a penetration tube and its through-hole is 0.2 mm (0.007 mils). The tube-to-wall weld only penetrates 7.6 mm (0.3 in) into the vessel wall, approximately 1/4 the total wall thickness.

The temperature and displacement histories of LHF-4 are shown in Figure 16. The heating history of the vessel was designed to be comparable to LHF-1. Due to a failure of heater zone 3, the actual heating rate was slightly slower than that of LHF-1. Creep initiation was observed 140 min into the experiment at a vessel temperature of approximately 930K. This temperature is consistent with the creep initiation temperature observed in LHF-1. The vessel developed a leak at 190 min into the experiment, at a vessel temperature between 970K (at 68° latitude) and 980K (at 90° latitude). The total deformation at the time of vessel failure was approximately 4 cm or about 8% strain. This is substantially smaller than the 12 cm, 25% strain observed in LHF-1.

Post-test examination indicated the failure occurred at penetration #9, located at 73° latitude, see Figure 17. The through-hole for the penetration was greatly enlarged, from 8.2 mm to a 1.3 mm by 1.6 mm oval. The neighboring penetrations at 68° latitude and 78° latitude also show similar through-hole deformation. It is interesting to note that these angles overlap the LHF-1 failure zone (66° to 80°). A comparison of the pre-test and post-test appearance of the weld indicates that failure occurred at the weld-fillet/vessel interface, see Figure 18. Apparently, the large global deformation of the vessel simply pulled apart the weld. Since Inconel has higher strength at elevated temperature, it is reasonable

that failure occurred at the weld fillet/vessel interface.

4.5 LHF-5 Experiment - Edge-Peaked Heat Flux with Penetrations

The LHF-5 experiment is designed to investigate the effect of penetrations on vessel failure with an edge-peaked heat flux distribution. There were nine scaled penetrations in the vessel bottom between latitudes 41° (highest penetration location for a PWR pressure vessel) and 80°. The selected installation locations represent the latitude range of penetration in a typical PWR. The installation also reproduces the maximum number of neighboring penetrations (3) to examine the possibility of the "postage rip effect" in a realistic geometry.

LHF-5 made use of an induction heated graphite radiating cavity located within the test vessel, see Figure 19. The cavity consists of a "top hat" supported on a 12.7 mm graphite base plate using 16, 8.9 cm high, 25-mm-diameter graphite spacers. The cylindrical section of the top hat is heated by induction. Thermal radiation escaped through the 8.9 cm gap between the rim of the top hat and the base plate is used achieve the edge-peak heat flux profile on the lower head.

The temperature, displacement, and pressure histories of LHF-5 are shown in Figure 20. The peak temperature is at 37° latitude. The peak to surrounding temperature contrast for LHF-5 is in the range of 200K; therefore, the normalized (with respect to yield stress at temperature peak) yield stress profile has a sharper minimum as compared to LHF-3, Figure 21. It appears that the test apparatus developed a slight leak at approximately 120 minutes into the experiment resulting in a gradual decrease in internal pressure from 9 MPa to 7.7 MPa at about 165 minutes. The pressure was brought up to the desired pressure of 10 MPa within 1.1 minutes. This increase in pressure resulted in a slight but noticeable (≈ 1 mm) response in the displacement transducer. Judging from the displacement measurement at 90°, vessel creep initiated at or slightly after the vessel pressure was increased to 10 MPa; the corresponding vessel temperature was 940K at 0° longitude and 1000K at 180° longitude. After creep initiation, the vessel continued to deform at an accelerated rate as the peak vessel temperature increased. The vessel ruptured at approximately 200 minutes into the experiment. The vessel temperature at failure was in the range of 1030K-1120K, with the maximum vessel temperature at 180° longitude. The overall vertical deformation at the time of failure was approximately 4 cm, comparable to the 5 cm observed in LHF-3.

As shown in Figures 22 and 23, the vessel failed with a horizontal rip at 37° latitude. The location of the rip appears to be coincidental with the circular locus of the peak temperature at 37° latitude. Post-test inspection indicated that vessel failure initiated at approximately 200° longitude quite near the region of maximum vessel temperature. The failure propagated in both directions for approximately 160° to 165°. Only the 5° to 40° section remained attached. The vessel thickness at the region of initial failure was between 3 mm and 4 mm, and increased monotonically along the tear, reaching approximately 11 mm near the termination of the tear. Both penetrations at 41° latitude (closest penetrations to the peak temperature location) suffered weld failure, see Figure 24. However, the penetrations were sufficiently far from the failure site, they were unlikely to have contributed to the failure.

4.6 Comparisons Between LHF-3 and LHF-5 Experiments

LHF-3 and LHF-5 both had side-peaked heat flux distribution. LHF-3 vessel failed with a partial rip and LHF-5 vessel was almost completely severed. The key difference is the relative magnitudes of hoop stress and the vessel yield stress at the time of creep initiation. The nominal hoop stress in the vessel wall for 10 MPa internal pressure is 75 MPa. At creep initiation LHF-3 was in the range of 960-970K; the corresponding yield stress is 120-127 MPa. In LHF-5, because of the delay in full pressurization, at creep initiation, the vessel temperature was in the range of 980-1025K, the corresponding yield stress was in the range of 70-110 MPa.

Perhaps it is reasonable to speculate that because of the sensitivity of creep to temperature:

Delaying the initiation of creep (or initiating creep by pressurization) until the vessel was well above previously observed temperature for creep initiation may have contributed to the nearly complete ripping of the bottom head.

5. SUMMARY of OBSERVATIONS from LHF-1 to LHF-5 EXPERIMENTS

- Localized heating results in localized failure.
- The failure size is typically smaller than the heated region.
- Temperatures for the initiation of failure and final failure appears to be fairly consistent.
- The wall thickness at failure appears to be fairly constant.
- It appears that the failure location might be related to slight variations in the manufacturing of the vessel.
- Vessel with penetration can fail prematurely as a result of weld failure due to the large strain associated with global deformation of the vessel.
- Pressure transients can have significant effects on vessel failure.

ACKNOWLEDGMENTS

This work was supported by the U.S. Nuclear Regulatory Commission, and was performed at Sandia National Laboratories. Sandia is a multiprogram laboratory operated by Sandia Corporation, A Lockheed Martin Company, for the U.S. Department of Energy under Contract DE-AC04-94AL85000.

REFERENCES

Chu, T.Y., M.M. Pilch and J.H. Bentz, "An Assessment of the Effects of Heat Flux Distribution and Penetration on the Creep Rupture of a Reactor Vessel Lower Head," Proceedings, ANS Winter Meeting, Albuquerque, NM, Nov., 1997.

Pilch, M.M., Rashid, Y.R., Ludwigsen, J.S., and Chu, T.Y., "Creep Failure of a Reactor Pressure Vessel Lower Head Under Severe Accident Conditions," Accepted for presentation at ASME PVP Conference, San Diego, CA, July 26-30, 1998.

Stickler, L.A., J.L. Rempe, S.A. Chavez, G.L. Tinnes, S.D. Snow, R.J. Witte, M.L. Corradini and J.A. Kos, Calculations to Estimate the Margin to Failure in the TMI-II Vessel, OECD-NEA-TMI-II Vessel Investigation Project, TMI V(93) EG01, Idaho National Engineering Laboratory, Idaho Falls, ID, 1993.

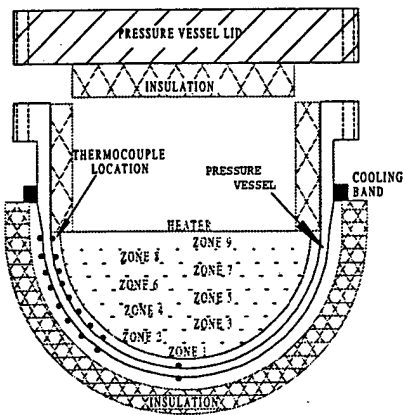


Figure 1. Schematic of LHF test apparatus.

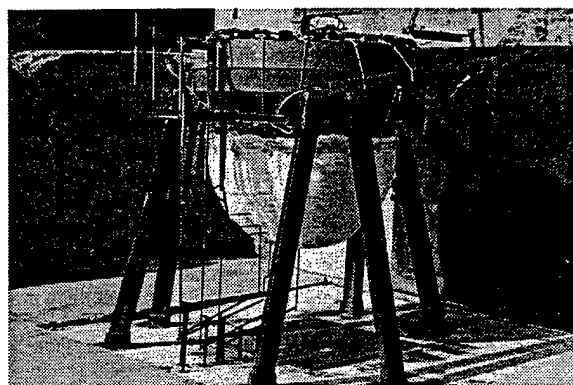


Figure 2. An overall view of the LHF test vessel and support.

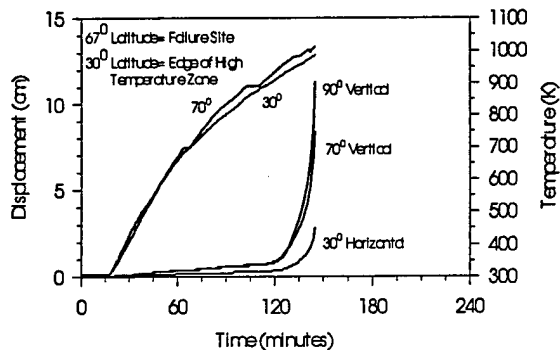


Figure 3. LHF-1 temperature and displacement history.

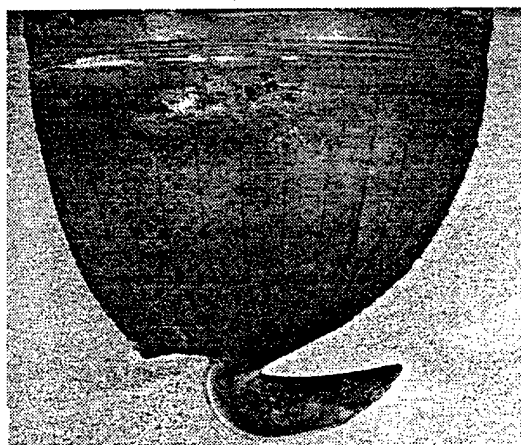


Figure 4. LHF-1 vessel profile 270° view - 180°/0° plane.

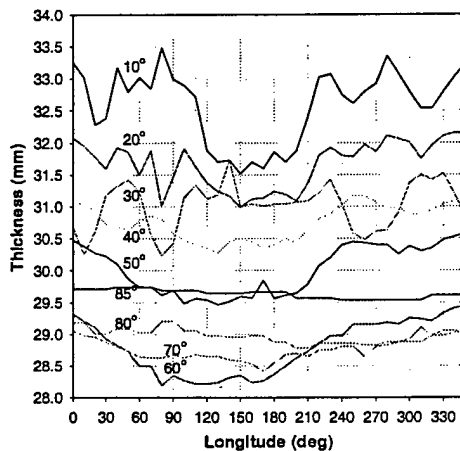


Figure 5. LHF-1 Pre-test thickness map (by latitudinal angle).

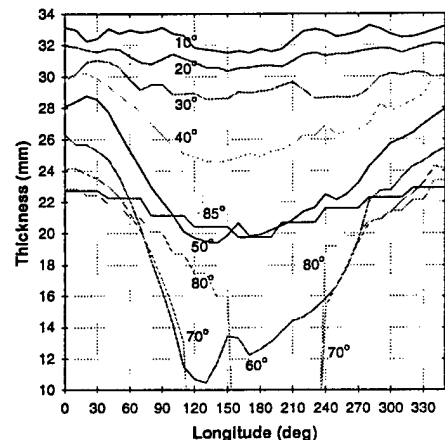


Figure 6. LHF-1 Post-test thickness map (by latitudinal angle).

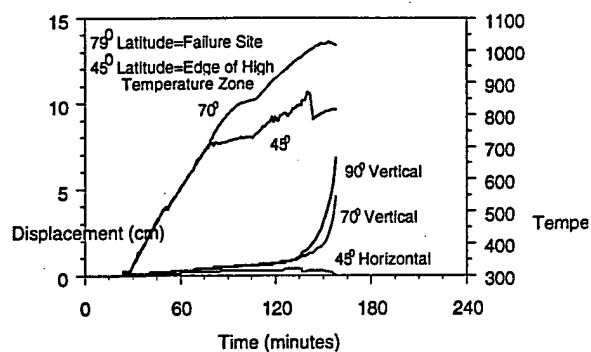


Figure 7. LHF-2 temperature and displacement history.

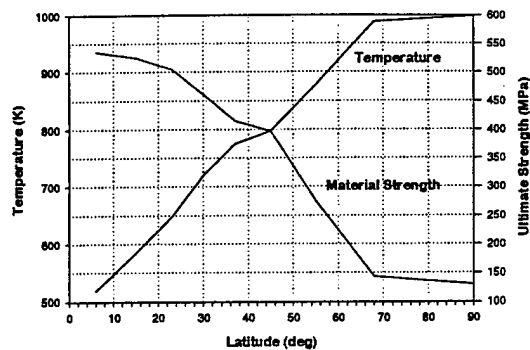


Figure 8. LHF-2 vessel temperature and strength profile.

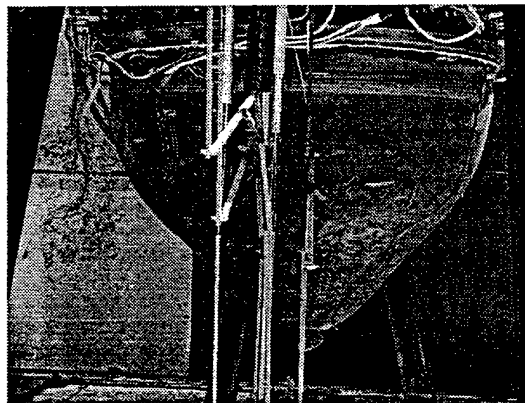


Figure 9. LHF-2 Vessel profile, 180° view - 90°/270° plane.

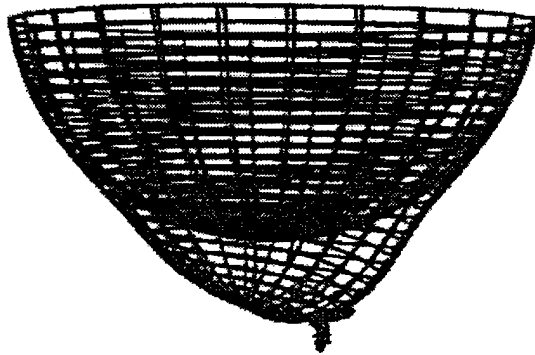


Figure 10. LHF-2 vessel deformation maps.

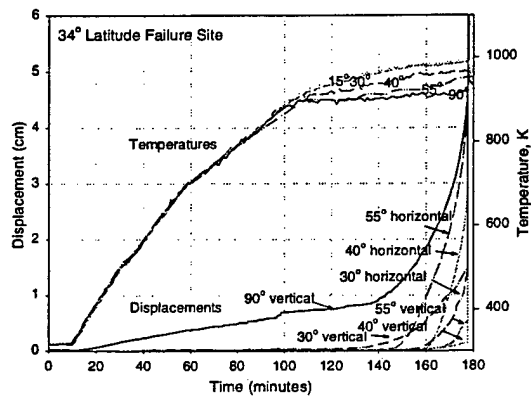


Figure 11. LHF-3 Temperature and displacement history (by longitudinal angle).

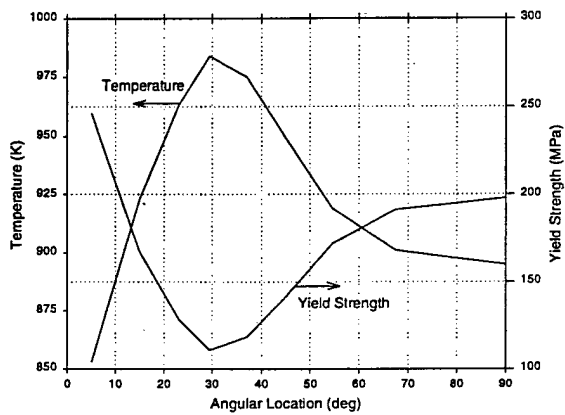


Figure 12. LHF-3 Yield strength Profile at 150 minutes.

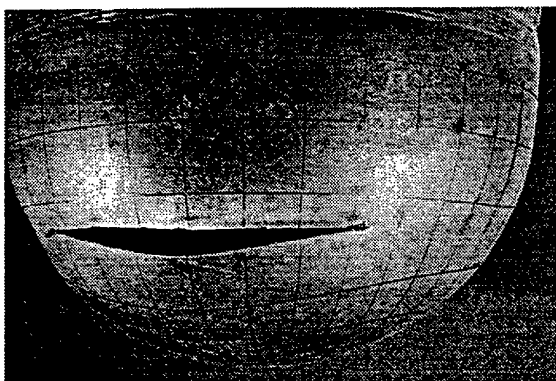


Figure 13. Close-up view of LHF-3 failure.



Figure 15. LHF-4 penetration pattern.

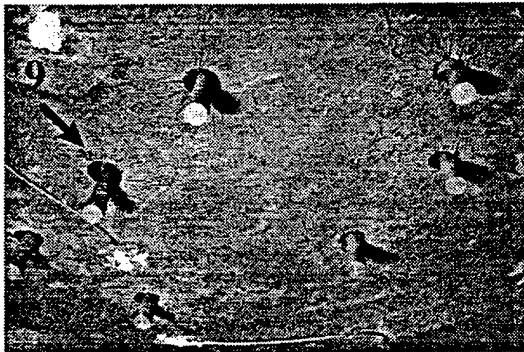


Figure 17. LHF-4 penetration through-hole enlargement.

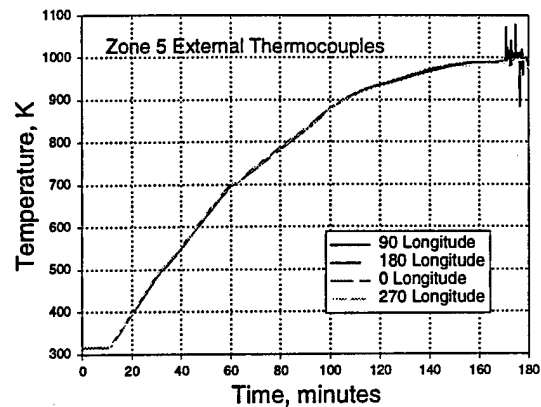


Figure 14. LHF-3 wall temperature history at four circumferential locations near the peak temperature region.

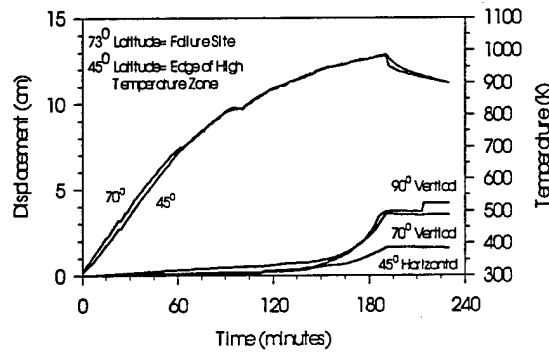


Figure 16. LHF-4 temperature and displacement history.

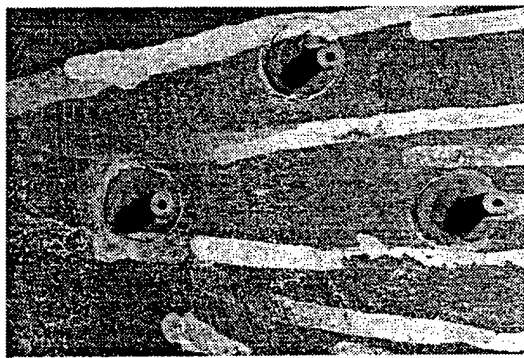


Figure 18. LHF-4 penetration weld (post-test).

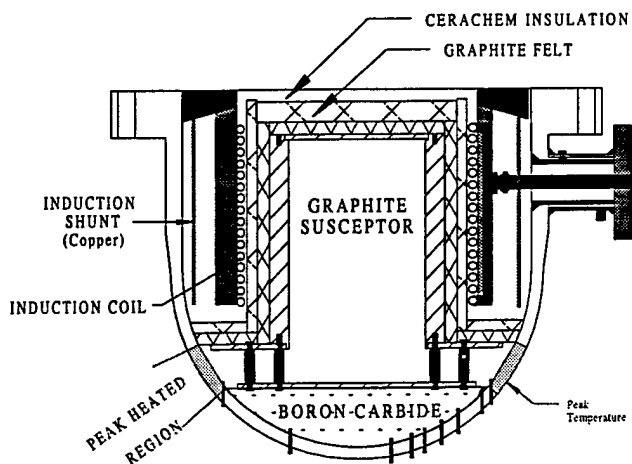


Figure 19. LHF-5 experimental design.

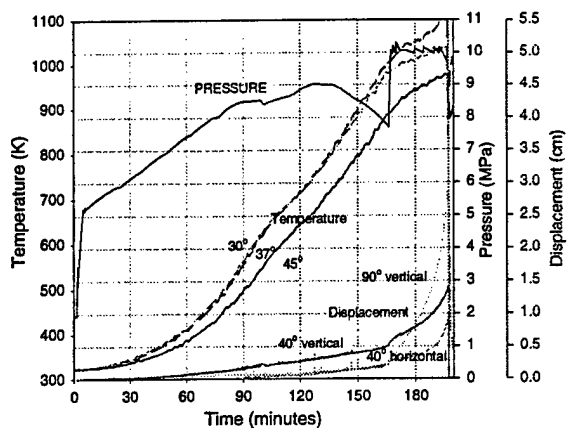


Figure 20. LHF-5 vessel Temperature (180° azimuth; 30°, 37°, and 45° latitude), internal pressure, and displacement history.

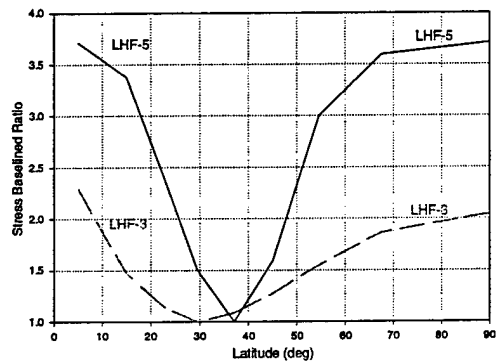


Figure 21. Comparison of latitudinal yield stress profile for LHF-3 and LHF-5.

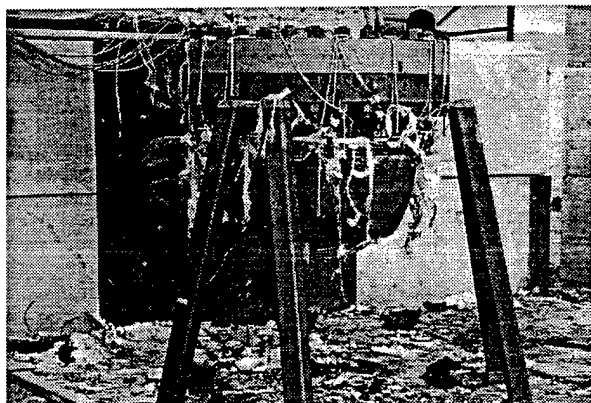


Figure 22. LHF-5 Post-test view.



Figure 23. LHF-5 Post-test view.

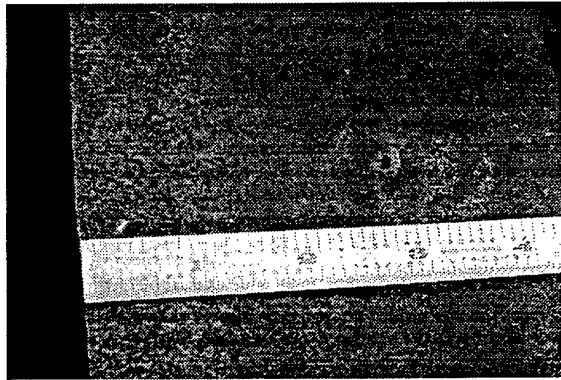


Figure 24. Penetration weld failure.

M98004098



Report Number (14) SAND--98-0580C
CONF-980341--

Publ. Date (11) 199803
Sponsor Code (18) NRC, XF
UC Category (19) UC-000, DOE/ER

DOE